Talanta 129 (2014) 282–289

Contents lists available at ScienceDirect

Talanta

journal homepage: www.elsevier.com/locate/talanta

Development of aptamer-conjugated magnetic graphene/gold nanoparticle hybrid nanocomposites for specific enrichment and rapid analysis of thrombin by MALDI-TOF MS

Ya Xiong, Chunhui Deng *, Xiangmin Zhang

Department of Chemistry and Institutes of Biomedical Science, Fudan University, Shanghai 200433, China

ARTICLE INFO

Article history:
Received 10 April 2014
Received in revised form
18 May 2014
Accepted 21 May 2014
Available online 6 June 2014

Keywords:
Aptamer
Magnetic graphene/gold nanoparticles nanocomposites
Selective enrichment
Thrombin detection
MALDI-TOF mass spectrometry

ABSTRACT

Simple, rapid and sensitive analysis of thrombin (a tumor biomarker) in complex samples is quite clinical relevant and essential for the development of disease diagnosis and pharmacotherapy. Herein, we developed a novel method based on aptamer-conjugated magnetic graphene/gold nanoparticles nanocomposites (MagG@Au) for specific enrichment and rapid analysis of thrombin in biological samples using MALDI-TOF-MS. At first, gold nanoparticles were compactly deposited on PDDA functionalized magnetic graphene through electrostatic interaction. Afterwards, aptamer was easily conjugated to gold nanoparticles via Au-S bond formation. The as-made aptamer-conjugated nanocomposites took advantage of the magnetism of magnetic graphene, the high affinity and specificity of aptamer, facilitating a high-efficient separation and enrichment of thrombin. More importantly, due to the large surface area of the hybrid substrate, the average coverage density of aptamer achieved 0.34 nmol/mg, which enhanced the thrombin binding capacity and the recovery of thrombin in real samples. In turn, the enriched thrombin attributed to the sensitive output of MALDI-TOF mass spectrometry signal, 0.085 ng μL^{-1} (2.36 nM) thrombin could be detected. This proposed method has a relatively wide linear relation ranging from 0.1 ng μL^{-1} to 10 ng μL^{-1}, and satisfactory specificity. The proposed high-throughput method based on MALDI-TOF MS is expected to the application in the disease biomarker detection and clinical diagnosis.

1. Introduction

Protein biomarkers are novel indicators of specific biological states and pathological conditions of certain diseases [1,2]. Thrombin has found to be a useful tumor biomarker for the diagnosis of pulmonary metastasis [3]. The detection of thrombin in the blood serum or routinely clinical tests is essential to disease diagnosis, therapy and prediction of therapeutic response [4]. Various methods have been applied in detecting thrombin, such as colorimetric [5], quantum dots [6], electrochemical [7,8], fluorescence [9,10], chemiluminescent [11], and surface enhanced Raman scattering (SERS) [12] methods. However, these methods are usually tedious, time consuming and have a very low throughput. Recently, matrix-assisted laser desorption ionization/time-of-flight mass spectrometry (MALDI-TOF-MS) with high speed and high throughput [13–15], was successfully developed to the analysis of thrombin in biological samples [16]. As thrombin has a very low concentration and serious interference with various non-target proteins or other coexistent substances in biological samples [17]. Therefore, highly selective enrichment of thrombin from complex samples is required prior to the MALDI-TOF-MS analysis.

Aptamer, as a recognition element, with numerous unique features, such as high binding affinity and specificity towards targets, standardized chemical synthesis with high purity at low cost, good stability, easy chemical modification, has been widely applied to high-selectivity enrichment of disease biomarkers [18,19]. In some previous reports, they generally introduced nanomaterials to anchor aptamers for thrombin enrichment [20]. For instance, Deng et al. developed organic-inorganic hybrid silica monolithic capillary column to immobilize aptamers, the limit detection of thrombin was 3.4 nM and the recovery of thrombin was 89.31 ± 5.6% [21]. The Tan's group employed (PEG)-modified gold nanorods to immobilize aptamers, 1 ppm sample of thrombin in buffer could be enriched with around 90% efficiency [22]. Zhang et al. synthesized chitosan modified Fe_3O_4 particles to immobilize aptamer, the limit detection of thrombin was 1 nM but the specific test involved only one non-target protein [23]. The above aptamer-conjugated nanomaterials provided a multifunctional platform to facilitate targeted recognition, enrichment and separation. Particularly, using magnetic nanomaterials as the substrate for aptamer immobilization led to separation and enrichment process simple

* Corresponding author. Fax: +86 21 65641740.
E-mail address: chdeng@fudan.edu.cn (C. Deng).

http://dx.doi.org/10.1016/j.talanta.2014.05.045
0039-9140/

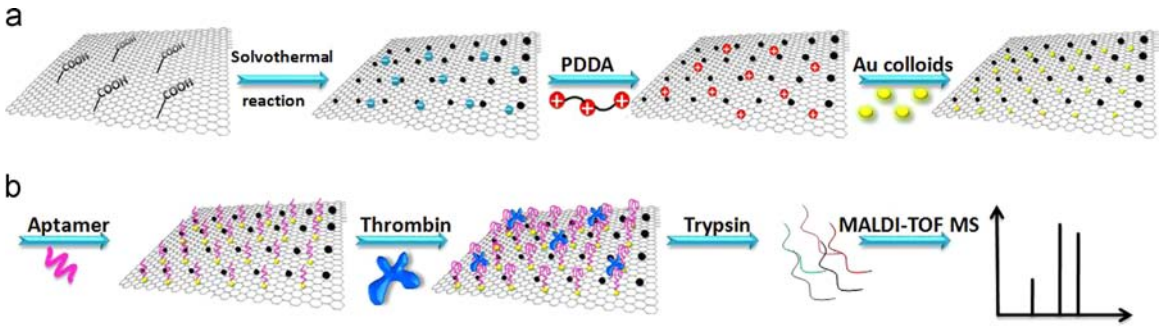

Scheme 1. Schematic illustration of (a) the preparation process of MagG@Au nanocomposites and (b) the process of aptamer immobilization and thrombin enrichment for MALDI-TOF MS analysis.

and rapid. Therefore, the outstanding features of nanomaterials play the key role in enrichment efficiency. However, current nanomaterials applied for aptamer immobilization exhibited poor water dispersibility, small surface area or laborious separation. Thus, developing the hybrid nanocomposites with good hydrophilicity and large surface area for aptamer immobilization for selective enrichment and rapid analysis of thrombin in samples is very interesting and important.

Graphene, owing to its ultrahigh surface area, non-covalently decorated with metal and metal oxide nanoparticles are considered extraordinary hybrid materials in nanobiotechnology [24]. Magnetic graphene which combines the advantage of magnetism for fast separation and the excellent properties of graphene, exhibited a good performance in small molecules, peptides, proteins enrichment and detection in our previous works [25–27]. In this work (Scheme 1), we developed magnetic graphene/Au hybrid nanocomposites with ultrahigh surface area for aptamer immobilization for highly specific enrichment and rapid analysis of thrombin using MALDI-TOF MS.

2. Experimental

2.1. Chemicals and reagents

The human α-thrombin binding aptamer (TBA), peptide ER-10 (ELVESYIDGR) and DF-8 (DRVYIHPF) were synthesized by Sangon Biotechnology Company (Shanghai, China). The sequence of TBA is 5′–SH-(CH2)6-TT TTT TTT TTG GTT GGT GTG GTT GG-3′. Human α-thrombin, human serum albumin (HSA), myoglobin, ribonuclease b, transferring, fetal calf serum, trifluoroacetic acid (TFA), α-cynano-4-hydroxycinnamic acid (CHCA), TPCK treated trypsin and polyelectrolyte poly (diallyldimethylammonium chloride) (PDDA) were purchased from Sigma. Tris (2-carboxyethyl) phosphine hydrochloride (TCEP) was purchased from Alfa Aesar. Human serum was donated by healthy people from Zhongshan Hospital (Shanghai, China). Ultrapure water (18.2 MΩ cm) was purified by a Milli-Q system (Millipore, Bedford, MA).

2.2. Synthesis of MagG@Au nanocomposites

Briefly, the magnetic graphene was prepared via a solvothermal approach reported in our previous works [25]. 13 nm gold colloids were prepared using a typical method according to previous report [16]. Then, the as-prepared magnetic graphene were dispersed into an aqueous solution of 0.20% PDDA containing 20 mM Tris base and 20 mM NaCl by stirring for 20 min. The PDDA attached materials were rinsed with water three times. Finally, three 100 mL as-prepared gold colloids were added under vigorous stirring at 1 h intervals. The obtained MagG@Au composites were washed with deionized water three times and dried under vacuum at 60 °C for 6 h.

2.3. Apparatus and characterization

The morphologies of nanocomposites were investigated by scanning electron microscopy with an energy dispersive X-ray (EDX) characterization (ESEM, Model XL 30 ESEM FEG from Micro FEI Philips) and transmission electron microscopy (JEOL 2011, Japan). The concentration of DNA was measured by a SHIMADZU Uvmini-1240 spectrometer system at 260 nm.

2.4. Immobilization of TBA onto MagG@Au nanocomposites

The thiolated aptamer directly conjugated with MagG@Au nanocomposites were prepared as follows: 6.75 nmol TBA was pretreated with 2.5 mM TCEP and 500 mM acetate buffer (pH5.2) for 1 h. Afterwards, MagG@Au nanocomposites were incubated with TCEP-activated TBA for 16 h at room temperature in the dark. The TBA functionalized MagG@Au conjugates was washed with binding buffer (10 mM PBS, 10 mM Na_2HPO_4, 2 m MKH_2PO_4, 137 m MNaCl, 2.7 mM KCl, 1 mM $MgCl_2$, 1 mM $CaCl_2$, PH 7.4) with the help of a magnet and stored in Tris–HCl buffer (50 mM Tris base, 100 mM NaCl, pH 8.0) at 4 °C for further use.

2.5. Enrichment of thrombin and MALDI-TOF MS analysis

A series of mixtures (50 μL of bulk solutions) of various concentration thrombin (0.1 ng μL^{-1}–250 ng μL^{-1}) and appropriate amount of MagG@Au@TBA conjugates in the binding buffer were equilibrated under vigorous shaking at room temperature for 1 h. The above bioconjugates were washed with PBS and 25 mM NH_4HCO_3 buffer successively to remove unbounded species. Thereafter, the mixture resuspended with NH_4HCO_3 buffer was heated at 100 °C for 30 s and treated with trypsin for digestion overnight at 37 °C. Lastly, 1 μl supernatant of analyte was pipette onto a MALDI target plate, followed by 20 pg of peptide DF-8 or 200 pg of peptide ER-10 as the internal standard and 0.5 μL of CHCA (4 mg/mL, 50% ACN, 0.1% TFA) as the matrix for mass spectrometry analysis.

For application of TBA-conjugated MagG@Au nanocomposites to real sample, various concentration of thrombin was added to 10-fold diluted human serum solution for 1 h incubation. Then, the above bioconjugates were washed with binding buffer containing 0.1% Tween-20 to remove any nonspecific binding. The following analytical processes were the same as those in the standard solutions.

Mass spectrometry analysis was performed a in reflection mode on a 5800 Proteomics Analyzer (Applied Biosystems, Framingham, MA, USA) with the Nd:YAG laser at 355 nm, a repetition rate of 200 Hz and an acceleration voltage of 20 kV.

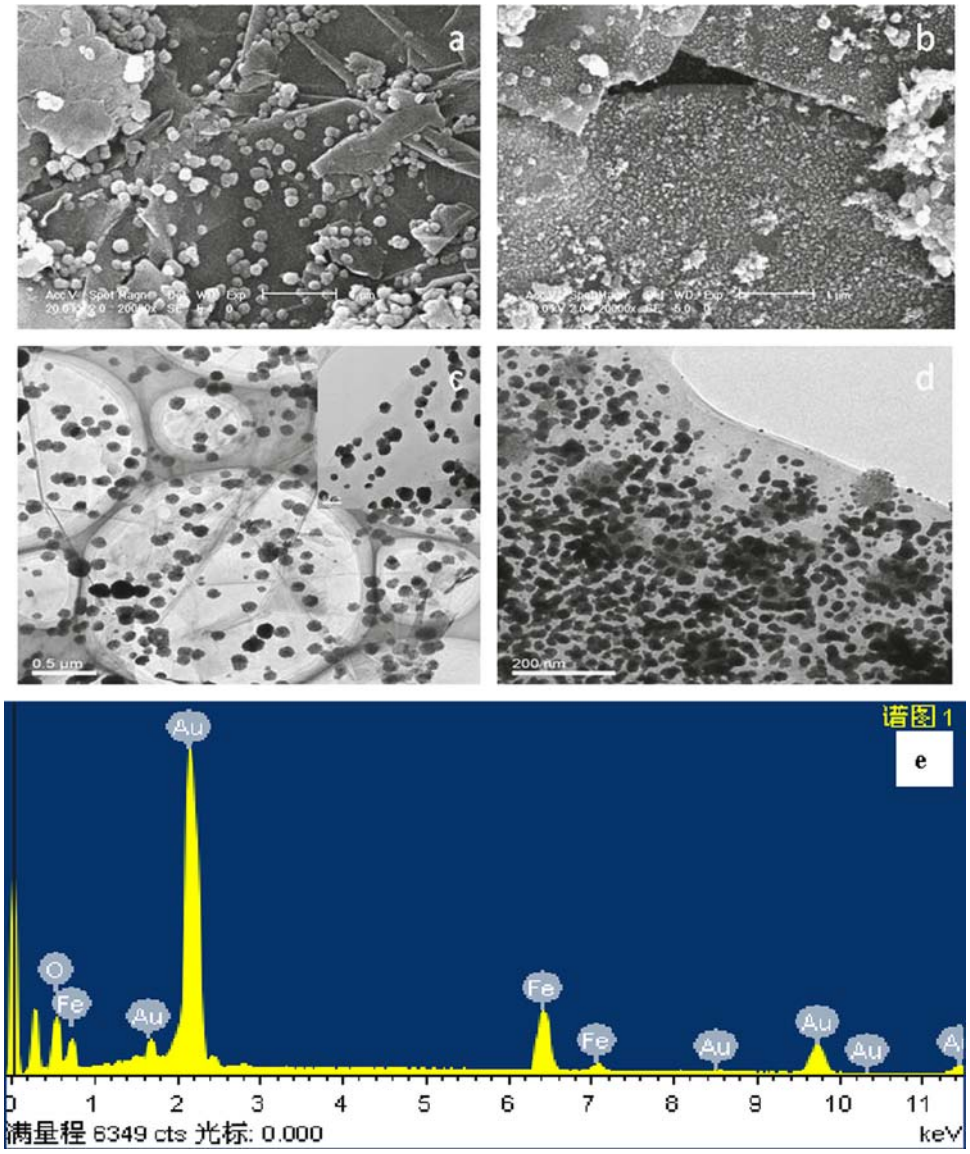

Fig. 1. The SEM images of (a) magnetic graphene and (b) MagG@Au nanocomposites. The TEM images of (c) magnetic graphene and (d) MagG@Au nanocomposites. The energy dispersive X-ray (EDX) spectrum of MagG@Au nanocomposites (e).

3. Results and discussion

3.1. Fabrication of TBA-conjugated MagG@Au nanocomposites

Scheme 1a illustrates the preparation process of MagG@Au nanocomposites. Magnetic graphene were easily synthesized via a solvothermal reaction. Specifically, the surface of graphene nanosheets was negatively charged and formed enormous hydrophilic groups like hydroxyl and carboxyl after treated with oxidative nitric acid. Then we introduced positive charged PDDA for deposition of gold nanoparticles through electrostatic interaction. The morphologies of magnetic graphene and MagG@Au nanocomposites were verified by SEM and TEM. The SEM and TEM images of the magnetic graphene (Fig. 1a and c) demonstrate that the orderly spherical magnetite beads were highly dispersed on the graphene nanosheets. Here, the utilization of an external magnetic field allowed for an easy separation as well as preconcentration of the analyte [28]. As we know, the excellent properties of gold nanopaticles allowed them immobilizing aptamers easily via Au-s bond formation [29,30]. Moreover, aptamer-conjugated gold nanoparticles exhibit multivalency, biocompatibility, resistance against nuclease digestion and improve binding affinity toward thrombin [31–33]. We can see in Fig. 1b and d that a condense layer of gold nanoparticles generated on the magnetic graphene surface. The energy-dispersive X-ray analysis also confirms the existence of Fe, Au elements (Fig. 1e). The as-prepared MagG@Au nanocomposites with large surface area and high-density hydrophilic groups remarkably amplified the loading amount of aptamer for signal amplification [34]. The average coverage density of aptamer reached 0.34 nmol/mg (RSD = 12.5%, $n = 3$). This result indicated that the developed MagG@Au hybrid nanocomposites constituted as a novel platform for immobilization of thrombin binding aptamer with high capacity.

3.2. Feasibility test using TBA-conjugated MagG@Au nanocomposites

TBA is a well-characterized DNA aptamer that folds into an unparallel G- quadruplex when it binds thrombin with high affinity ($K_d = 0.5$ nmolL^{-1}) [35]. This kind of unparallel G- quadruplex structure could be stabilized by K^+ ion, Na^+ ion, Mg^{2+} ion, Ca^{2+} ion etc.

[36–38]. Herein, 50 μL human α-thrombin (20 ng μL^{-1}) was incubated with TBA-conjugated MagG@Au nanocomposites in PBS buffer. After reached equilibrium, thrombin was selectively enriched with fast magnet separation. Thermal denaturation is a simple method for protein and nucleic acid denaturation. The above mixture resuspended with NH_4HCO_3 buffer was heated at 100 °C for 30 s, during which both specific secondary structures of thrombin and aptamer undergone conformation switching and unfolding processes, contributing to thrombin releasing and efficient tryptic digestion [39]. Finally, generated peptides were analyzed by MALDI-TOF MS. Fig. 2 shows a representative MALDI-TOF mass spectrum performed after enrichment and trypsin digestion of thrombin at 20 ng μL^{-1}. The strongest peak marked with asterisk was chosen as signal peptide for data statistics. This result shows that our proposed method is feasible, simple and rapid.

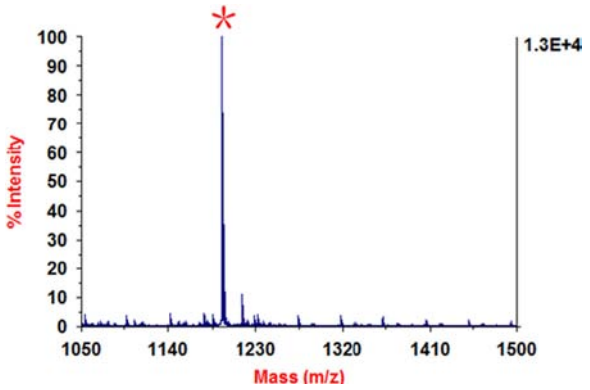

Fig. 2. A representative MALDI-TOF mass spectrum performed after enrichment and trypsin digestion of thrombin at 20 ng μL^{-1}. The signal peptide (m/z=1194.6) was marked by asterisk.

3.3. Quantitative detection of thrombin

Typical results obtained from four replicate analysis of thrombin were shown in Fig. 3. To further evaluate our method could quantitatively detection of thrombin, the analysis of thromin in a dynamic concentration range from 0.1 ng μL^{-1} to 250 ng μL^{-1} was measured. It has been reported that an internal standard was essential for MALDI-TOF MS quantitative measurements in precision and in accuracy [40]. We employed peptide DF-8 (m/z=1046.6) with sequence DRVYIHPF as the internal standard [16]. The plot of the logarithm of intensity ratio of 1194.6 versus 1046.6 against the logarithm of the concentration of thrombin performed a good linear positive correlation with R^2=0.988 in the range of 0.1 ng μL^{-1} to 10 ng μL^{-1} (Fig. 4a), and the intensity of signal peptide gone down promptly when concentration of thrombin was larger than 50 ng μL^{-1}(Fig. 4b). The detection limit of thrombin was calculated to be 0.085 ng μL^{-1} according to three times standard deviation of blanks. When the concentration of thrombin was as low as 0.085 ng μL^{-1} (2.36 nM), the signal peak of m/z 1194.6 could still be distinguished from the background with signal-to-noise ratio of larger than 10 (Fig. 4c).

3.4. Specificity of TBA-conjugated MagG@Au nanocomposites to thrombin

We further validated the specificity by the aptameric recognition function. Four unmatched proteins including HSA, Myoglobin, Ribonuclease b, Transferrin and a biological sample fetal calf serum, at concentration of 100 ng μL^{-1}, 20-fold of thrombin (5 ng μL^{-1}), were used instead of thrombin, no target signal are appeared in the whole mass spectrum (Fig. 5a). However, the perfectly matched target thrombin reveals so much high signal response that the other interference is negligible. Even the biological sample fetal calf serum did not interfere with the determination for a trace amount (5 ng μL^{-1}) of thrombin

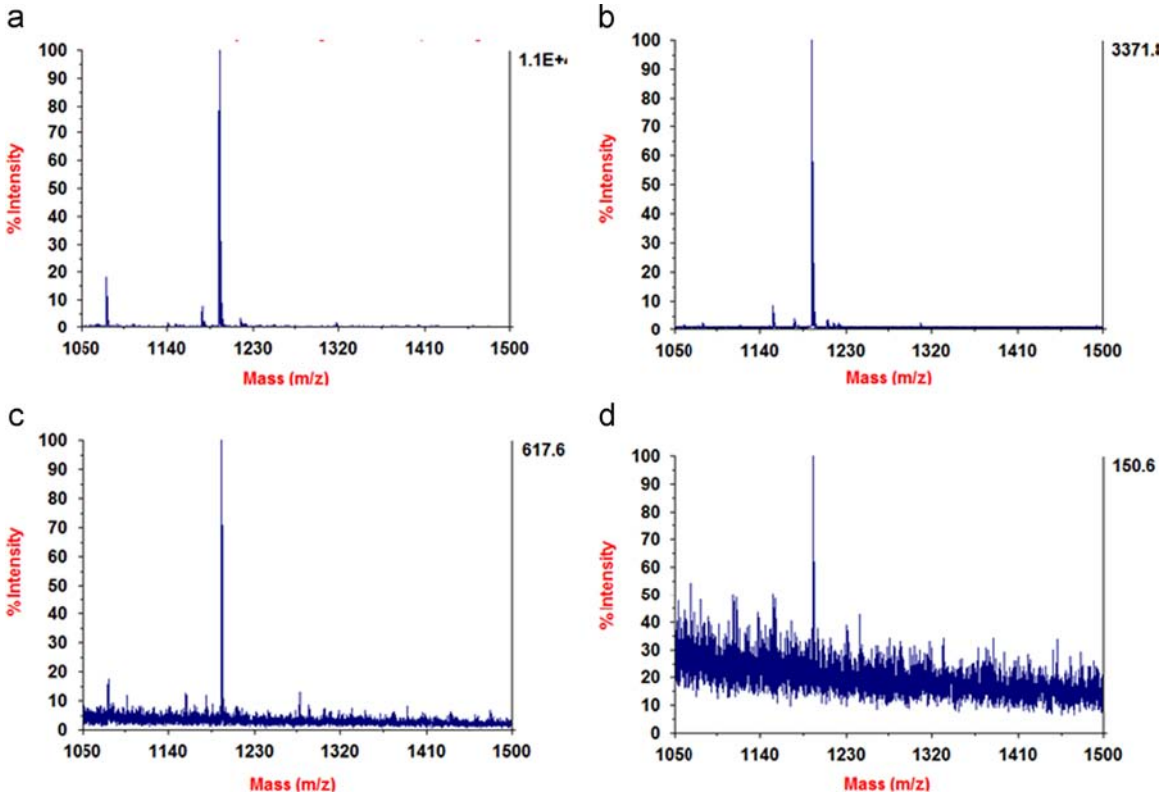

Fig. 3. Detection of thrombin in standard solutions with different concentrations, (a) 25 ng μL^{-1} (b) 10 ng μL^{-1} (c) 1 ng μL^{-1} and (d) 0.1 ng μL^{-1}.

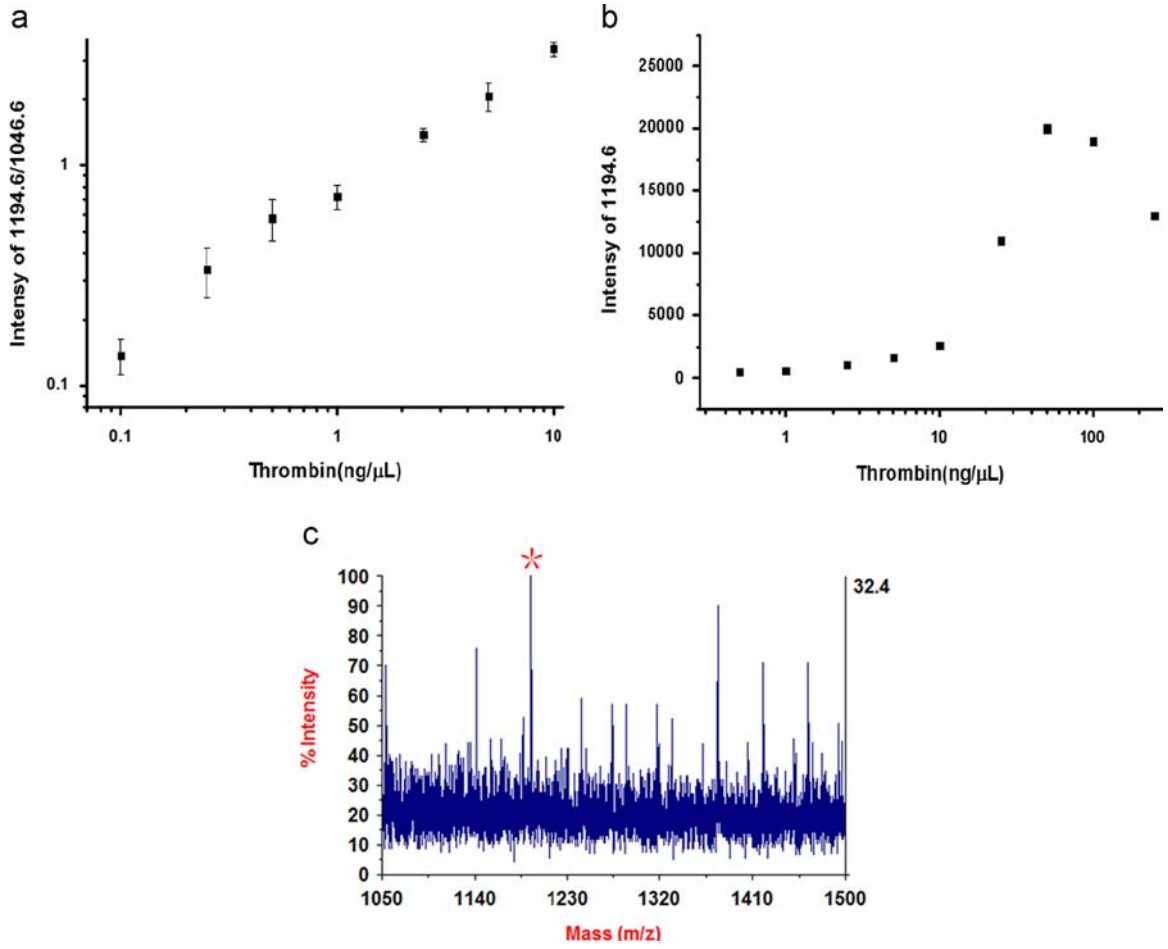

Fig. 4. (a) Linear relationship between the MS intensity of the signal peptide and concentrations of thrombin. The linear equation is $Y=0.661X-0.123$. $R^2=0.988$. The error bars represent the standard deviation of three measurements; (b) The dynamic range of detection of thrombin in standard solutions; (c) The detection limit of thrombin was as low as 0.085 ng μL^{-1} (2.36 nM), the signal-to-noise ratio was 13.8.

(Fig. 5b). All these results demonstrate that thrombin could be selectively captured on TBA-conjugated MagG@Au nanocomposites by the specific interaction between aptamer and human α-thrombin. The high specificity of our assay holds a great promise for application in complex samples.

3.5. *Application of TBA-conjugated MagG@Au nanocomposites to real sample*

The level of thrombin circulates higher in the blood of patients than health people, thus it is significant to test thrombin in real blood serum for medical diagnosis [41,42]. However, the inhibitors in serum could result in a low recovery of the spiked thrombin [43]. Appropriate dilution time of serum not only reduced the complex background of the matrix but also enhanced the recovery approaching to 100% [44]. We spiked 10-fold diluted human serum with 1 ng μL^{-1}, 2.5 ng μL^{-1}, 5 ng μL^{-1} thrombin respectively. The results are shown in Fig. 6, an obvious peak at *m*/*z* 1194.6 was observed. Subsequently, this peak was submitted to MS/MS analysis. Through comparing the b ions and y ions with that from thrombin standard solutions, this peak was indeed validated to belong to thrombin (data not shown). A peptide ER-10(ELVE-SYIDGR) differs one amino acid with the target peptide (ELLE-SYIDGR) was chosen as the internal standard [16]. Table 1 displays the recoveries of thrombin from 10-fold diluted human serum, demonstrating the practicability of our assay in real blood serum.

4. Conclusions

In this work, we successfully developed aptamer-conjugated magnetic graphene/gold nanoparticles nanocomposites for specific enrichment and rapid analysis of thrombin in biological samples using MALDI-TOF-MS. The aptamer-conjugated nanocomposites own several superiorities: (1) magnetic graphene/gold nanoparticles nanocomposites with ultrahigh surface area can serve as a multifunctional substrate to anchor aptamer with high capacity; (2) the magnet field facilitates a high-efficient enrichment and separation of thrombin; (3) aptamer offers high binding affinity and specificity towards thrombin. Benefited from the above superiorities as well as the strength of MALDI-TOF MS, we have achieved high sensitivity with relatively wide linear relation, satisfactory specificity that even real samples don't interfere with our assay, and good recovery of thrombin from human serum. We demonstrated that MALDI-TOF-MS technique combined with aptamer modified nano-platfrom has the powerful ability for rapid analysis of protein biomarkers in biofluids.

Novelty

In this work, we developed a novel method based on aptamer-conjugated magnetic graphene/gold nanoparticles nanocomposites (MagG@Au) for specific enrichment and rapid analysis of thrombin in biological samples using MALDI-TOF-MS. At first, gold nanoparticles were compactly deposited on PDDA functionalized

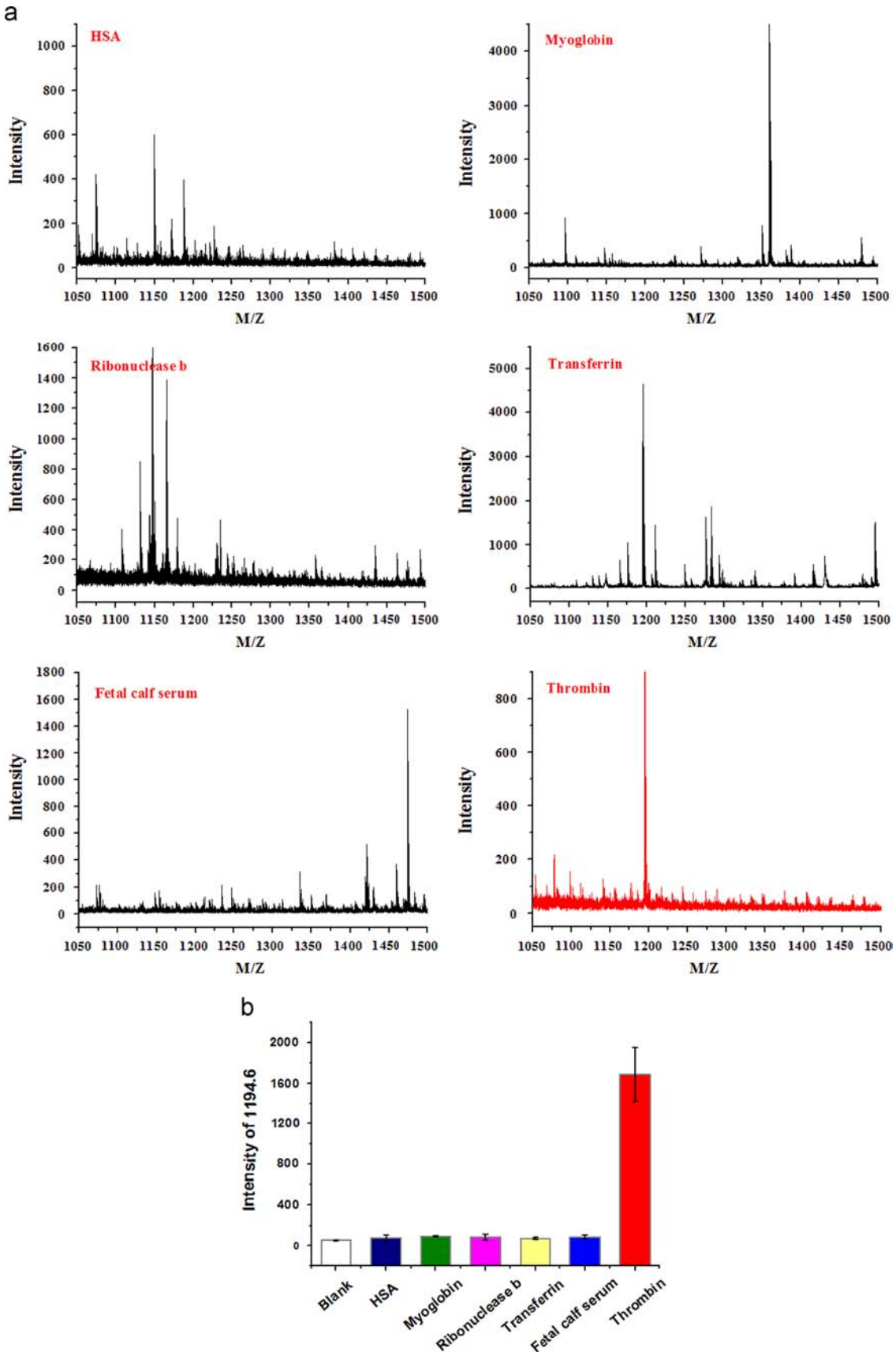

Fig. 5. (a) MALDI-TOF mass spectrums of five unmatched proteins and the target protein for specificity studies; (b) Specificity of the proposed assay for thrombin detection: HSA, Myoglobin, Ribonuclease b. Transferrin and a biological sample fetal calf serum were 100 ng μL^{-1}, thrombin was 5 ng μL^{-1}.

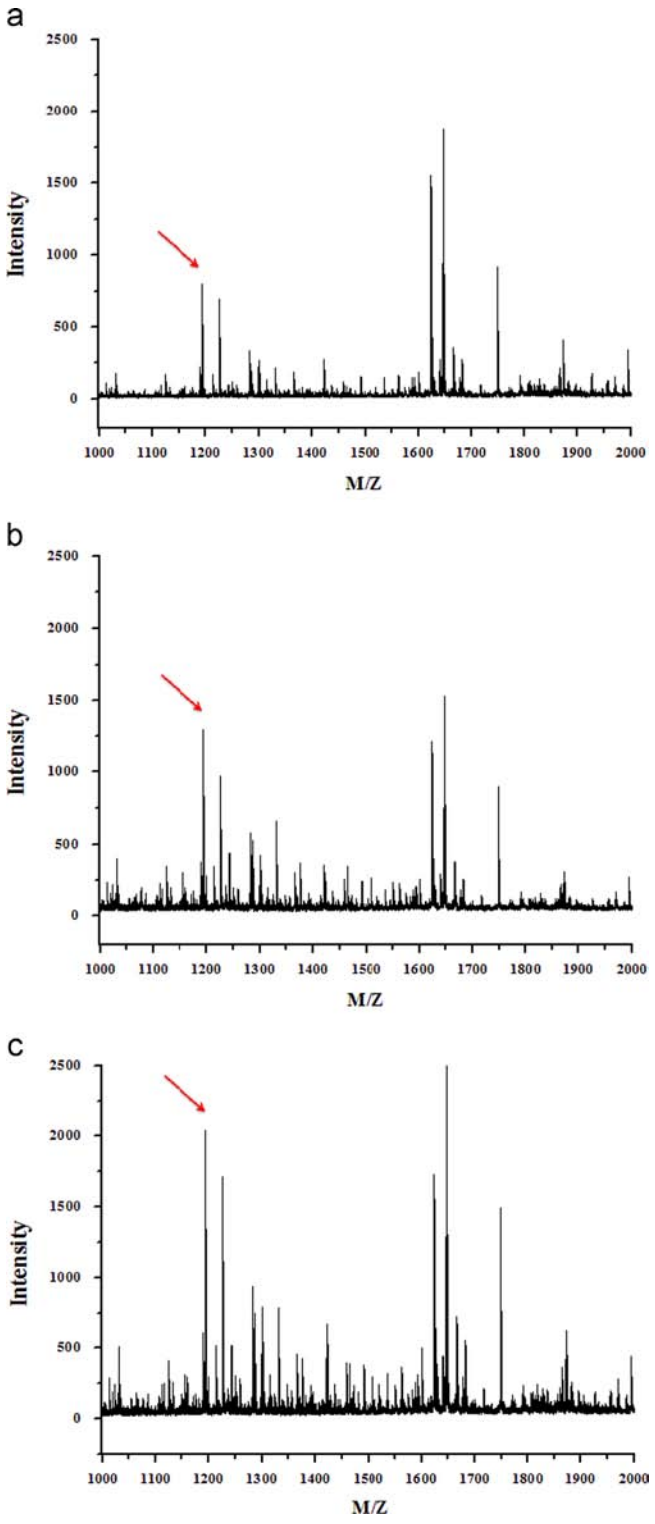

Fig. 6. The detection in 10-fold diluted human serum samples spiked with thrombin at (a) 1 ng μL^{-1} (b) 2.5 ng μL^{-1} (c) 5 ng μL^{-1}. Arrows points the peak m/z=1194.6.

magnetic graphene through electrostatic interaction. Afterwards, aptamer was easily conjugated to gold nanoparticles via Au-S bond formation. The as-made aptamer-conjugated nanocomposites took advantage of the magnetism of magnetic graphene, the high affinity and specificity of aptamer, facilitating a high-efficient separation and enrichment of thrombin. More importantly, due to the large surface area of the hybrid substrate, the average coverage density of aptamer achieved 0.34 nmol/mg, which enhanced the thrombin binding capacity and the recovery of thrombin in real samples. In turn, the enriched thrombin attributed to the sensitive output of MALDI-TOF mass spectrometry signal, 0.085 ng μL^{-1} (2.36 nM) thrombin could be detected. This proposed method has a relatively wide linear relation ranging from 0.1 to 10 ng μL^{-1}, and satisfactory specificity. The proposed high-throughput method based on MALDI-TOF MS is expected to the application in the disease biomarker detection and clinical diagnosis.

Table 1
The recovery of thrombin from 10-fold diluted human serum.

Spiked thrombin (ng μL^{-1})	Found (ng μL^{-1})	Recovery (%)	RSD (%)
1	1.07	107	7
2.5	2.39	95.6	9
5	5.24	104.8	15

Acknowledgments

This work was supported by the National Basic Research Priorities Program (2012CB910602, 2013CB911201), the National Natural Science Foundation of China (21075022, 21275033, 21105016), Research Fund for the Doctoral Program of Higher Education of China (20110071110007 and 20100071120053), Shanghai Municipal Natural Science Foundation (11ZR1403200) and Shanghai Leading Academic Discipline Project (B109).

References

[1] Y. Hu, D.H. Fine, E. Tasciotti, A. Bousmrani, M. Ferrari, Wiley Interdiscip. Rev.: Nanomed. Nanobiotechnol. 3 (2011) 11.
[2] N. Fifai, M.A. Gillette, S.A. Carr, Nat. Biotechnol. 24 (2006) 971.
[3] M.L. Nierodzik, S. Karpatkin, Cancer Cell 10 (2006) 355.
[4] H.J. Lee, E.Y. Lee, M.S. Kwon, Y.K. Paik, Curr. Opin. Chem. Biol. 10 (2006) 42.
[5] J. Nie, Y. Deng, Q.P. Deng, D.W. Zhang, Y.L. Zhou, X.X. Zhang, Talanta 106 (2013) 309.
[6] X.Y. Zhang, R.X. Hu, N. Shao, Talanta 107 (2013) 140.
[7] Z.J. Ya, Z.J. Han, H.Y. Huang, H.Y. Shen, X.J. Lu, Anal. Biochem. 442 (2013) 237.
[8] Z.H. Xu, C. He, T. Sun, L. Wang, Electroanalysis 25 (2013) 2339.
[9] M. Wang, C.Y. Lei, Z. Nie, M.L. Guo, Y. Huang, S.Z. Yao, Talanta 116 (2013) 468.
[10] L.Y. Xue, X.M. Zhou, D. Xing, Anal. Chem. 84 (2012) 3507.
[11] X.Y. Yang, A.G. Wang, J.L. Liu, Talanta 114 (2013) 5.
[12] C.V. Pagba, S.M. Lane, H.S. Cho, S. Wanchsmann-Hogiu, J. Biomed. Opt. 15 (2010) 047006.
[13] C.Y. Shi, C.H. Deng, S.E. Zou, X.M. Zhang, Talanta 127 (2014) 88.
[14] S.S. Liu, H.M. Chen, X.H. Lu, C.H. Deng, X.M. Zhang, P.Y. Yang, Angew. Chem. Int. Ed. 49 (2010) 7557.
[15] X.Y. Zhang, S.C. Zhu, Y. Xiong, C.H. Deng, X.M. Zhang, Angew. Chem. Int. Ed. 125 (2013) 6171.
[16] X.Y. Zhang, S.C. Zhu, C.H. Deng, X.M. Zhang, Talanta 88 (2012) 295.
[17] S. Centi, S. Tombelli, M. Minunni, M. Mascini, Anal. Chem. 79 (2007) 1466.
[18] A.B. Iliuk, L.H. Hu, W.A. Tao, Anal. Chem. 83 (2011) 4440.
[19] M. Mascini, I. Palchetti, S. Tombelli, Angew. Chem. Int. Ed. 51 (2012) 1316.
[20] L. Yang, X.B. Zhang, M. Ye, J.H. Jiang, R.H. Yang, T. Fu, Y. Chen, K.M. Wang, C. Liu, W.H. Tan, Adv. Drug Deliv. Rev. 63 (2011) 1361.
[21] N. Deng, Z. Liang, Y. Liang, Z.G. Sui, L.Y. Zhang, Q. Wu, K.G. Yang, L.H. Zhang, Y.K. Zhang, Anal. Chem. 84 (2012) 10186.
[22] E Yasun, B. Gulbakan, I. Ocsoy, Q. Yuan, M.I. Shukoor, C.M. Li, W.H. Tan, Anal. Chem. 84 (2012) 6008.
[23] Z.X. Zhang, Z.J. Wang, X.L. Wang, X.R. Yang, Sens. Actuators B 147 (2010) 428.
[24] C.N.R. Rao, A.K. Sood, K.S. Subrahmanyam, A Govindaraj, Angew. Chem. Int. Ed. 48 (2009) 7752.
[25] C.Y. Shi, J.R. Meng, C.H. Deng, Chem. Commun. 48 (2012) 2418.
[26] J. Lu., C.H. Deng, X.M. Zhang, P.Y. Yang, ACS Appl. Mater. Interfaces 5 (2013) 7330.
[27] M. Zhao, C.H. Deng, X.M. Zhang, ACS Appl. Mater. Interfaces 5 (2013) 7770.
[28] E. Temur, A. Zengin, I.H. Boyaci, F.C. Dudak, H. Torul, Anal. Chem. 84 (2012) 10600.
[29] S.V. Kumar, N.M. Huang, H.N. Lim, M. Zainy, I. Harrison, C.J. Chia, Sens. Actuators B 181 (2013) 885.
[30] L. Dykman, N. Khlebtsov, Chem. Soc. Rev. 41 (2012) 2256.
[31] Y.C. Shiang, C.L. Hsu, C.C. Huang, Angew. Chem. Int. Ed. 50 (2011) 7660.

[32] Y. Wu, J.A. Phillips, H. Liu, R. Yang, W. Tan, ACS Nano 2 (2008) 2023.
[33] J.N. Zhang, B. Liu, H.X. Liu, X.B. Zhang, W.H. Tan, Nanomedicine 8 (2013) 983.
[34] Y. Wang, R. Yuan, Y.Q. Chai, Y. Yuan, L.J. Bai, Biosens. Bioelectron. 38 (2012) 50.
[35] Y. Liu, C.X. Lin, H.Y. Li, H. Yan, Angew. Chem. Int. Ed. 44 (2005) 4333.
[36] R.F. Macaya, P. Schultze, F.W. Smith, J.A. Roe, J. Feigon, Proc. Natl. Acad. Sci. 90 (1993) 3745.
[37] A.H. Liang, J.S. Li, C.N. Jiang, Z.L. Jiang, Bioprocess Biosyst. Eng. 33 (2010) 1087.
[38] L. McFail-Islom, X. Shui, L.D. Williams, Biochemistry 37 (1998) 17105.
[39] Y. Koh, B.R. Lee, H.J. Yoon, Y.H. Jiang, Y.S. Lee, Y.K. Kim, B.G. Kim, Anal. Bioanal. Chem. 404 (2012) 2267.
[40] E. Szäjli, T. Feher, K.F. Medzihradszky, Mol. Cell Proteomics 7 (2008) 2410.
[41] J. Bichler, J.A. Heit, W.G. Owen, Thromb. Res. 84 (1996) 289.
[42] J. Müller, T. Becher, J Braunstein, P. Berdel, S. Gravius, F. Rohrbach, J. Oldenburg, G. Mayer, B. Pötzsch, Angew. Chem. Int. Ed. 50 (2011) 6075.
[43] Q. Zhao, X.F. Li, X.C. Le, Anal. Chem. 83 (2011) 9234.
[44] Y.C. Huang, B. Ge, D. Sen, H.Z. Yu, J. Am. Chem. Soc. 130 (2008) 8023.